Highly Conducting Patterned Pd Nanowires by Direct-Write Electron Beam Lithography

T. Bhuvana and G. U. Kulkarni*

Chemistry and Physics of Materials Unit and DST Unit on Nanoscience, Jawaharlal Nehru Centre for Advanced Scientific Research, Jakkur P.O., Bangalore 560 064, India

ARTICLE

ABSTRACT Palladium hexadecylthiolate is shown to serve as a negative-tone direct-write electron resist to produce nanopatterns down to 30 nm. The written patterns do not deviate much from the precursor in composition, while a post-treatment at 230 °C in air produced metallic Pd nanowires with residual carbon less than 10% and resistivity close to the bulk value, a desirable property of interconnects in nanocircuitry. The as-written patterns contain small nanocrystals (<5 nm) in a hydrocarbon matrix, which upon annealing aggregate to form well-connected networks of larger nanocrystals (5–15 nm), thus giving rise to metallic conductivity.

KEYWORDS: nanopatterning · electron beam lithography · metal nanowire · interconnects · electrical conductivity · thermolysis

Advancement in nanoelectronics crucially depends on the ease with which circuit elements based on nanomaterials can be fabricated reliably. This, in turn, has led to an intense activity in the literature, reporting innovative materials and methods to achieve below 100 nm fabrication.[1,2] An important and widely pursued aspect of nanopatterning is related to casting metals into submicrometer features and their exploitation as interconnects,[3–5] solder in nanocircuitry,[6,7] sensor elements,[8] or catalysts to grow nanotubes[9] and nanorods.[10] Charged particle beam-based lithography techniques, electron beam (EBL) and focused ion beam (FIB), are well suited, particularly when it comes to making an interconnect from a contact pad[3–5] or soldering a nano-object to it.[6,7] In this context, direct-write EBL or FIB methods employing metal precursor-based resist coatings,[11–18] or chemical vapor deposition under a focused beam (EBID[19–25] and FIBID[19,26–30]), find immense use. Tailor-made metal organic complexes and salts[11–13] as well as nanoparticle sols[14–18] have been employed as thin-film resists to generate nanopatterns of Au,[11,14–16] Ag,[16] Pd,[12,17,18] Co,[13] Ni,[13] and Mo[13] in direct-write methods. Vapor-phase precursors such as carbonyls of W,[19,26] Fe,[20] Cr,[20] and Mo as well as organometallic complexes of Pt[21–23,27–30] and Au[5,22,23] have been used in beam-induced depositions of the respective metals. One of the pertinent problems in such studies is that the written patterns invariably contain impurities from the starting precursor such as carbon and gallium, as much as 40% or even higher.[14,17,21–23,28–30] Often a post-treatment procedure is adopted to remove the organic impurity and improve the relative metal content,[12,14,17,21–23,26,27] albeit with an overall loss of metal because of the high temperature. Besides, the conducting property of the metal patterns is generally poor, the resistivity being usually a few orders of magnitude higher than that of the bulk,[12,14–23,26–30] except in cases where non-carbon-based precursors have been developed to obtain patterns with resistivity values a few times that of the bulk.[24,25]

We have made palladium nanopatterns by the direct-write EBL method using a novel resist, a palladium alkanethiolate. Pd being an important metal catalyst, its nanopatterning has attracted considerable attention.[8,10,12,17,18,31–34] Yan and Gupta[31] obtained 5 μm lines of Pd metal by UV-photodissociating an acetate film, while Lee *et al.*[10] exposed a patterned poly(methyl methacrylate) (PMMA) resist to the acetate vapor and produced Pd patterns down to 500 nm. By blending PMMA with Pd precursor, metallized polymer patterns have been obtained by both UV and EBL.[32] Microcontact printing has been used to create Pd metal nanostructures on substrates.[33] Patterned Pd was used for the catalytic growth of carbon nanotubes[9] and ZnO nanostructures,[10] as well as for electroless deposition of Cu.[34] Pd nanowires of varying diameters have been obtained by electrodeposition and employed in hydrogen sensing.[8] Stark *et al.*[12] patterned

*Address correspondence to kulkarni@jncasr.ac.in.

Received for review November 17, 2007 and accepted January 25, 2008.

Published online February 13, 2008.
10.1021/nn700372h CCC: $40.75

© 2008 American Chemical Society

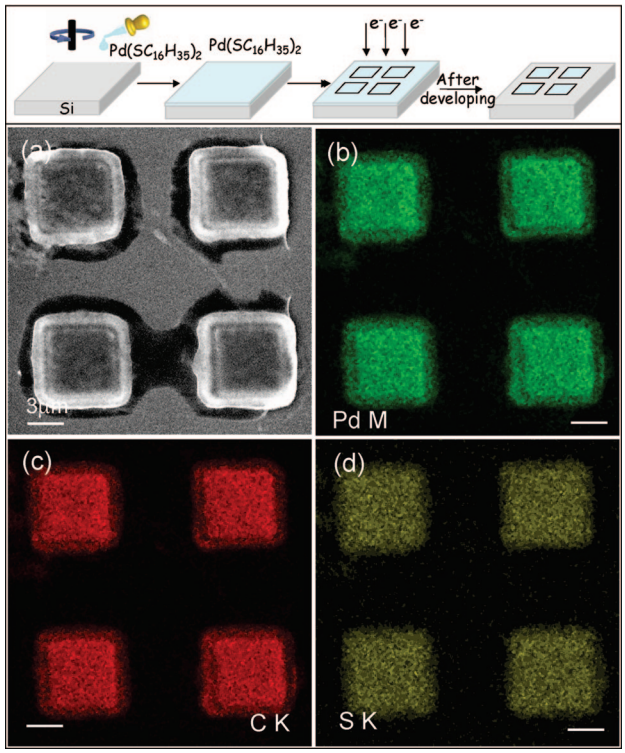

Figure 1. (Top) Schematic of the procedure adopted: step 1, spin-coating of the palladium hexadecylthiolate on Si(111) surface; step 2, EBL patterning at 5 kV; and step 3, developing the patterned substrate in toluene for 10 s. (a) SEM image after electron beam patterning. (b–d) EDS maps of the patterned region: (b) Pd M, (c) C K, and (d) S K lines.

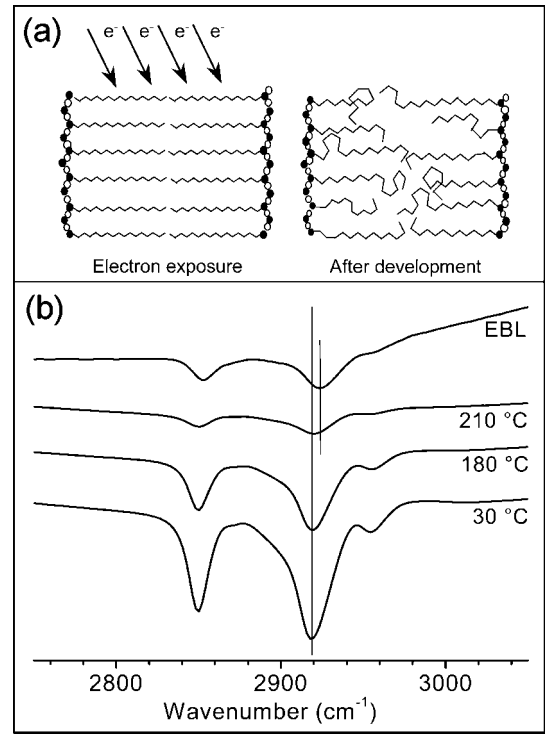

Figure 2. (a) Schematic showing the effect of electron beam exposure on the Pd hexadecylthiolate bilayer. (b) FTIR spectrum of a patterned film (3 × 3 mm^2) along with those obtained after subjecting a pristine film (without EBL) to different temperatures for 20 min.

palladium acetate with e-beam to get fine structures of Pd and studied their electrical properties. Reetz *et al.*[17] fabricated Pd and Pd/Pt nanostructures by exposing films containing corresponding cluster species to high dosages, ~0.2 C/cm^2 at 120 kV. These studies[12,17,18] report resistivity values which are a few orders of magnitude higher than that of the bulk Pd, mainly because of the carbon impurity. Here, we report how, in direct-write EBL, palladium hexadecylthiolate can be made to serve as a resist requiring low e-dosages, yet leading to highly conducting Pd nanopatterns.

RESULTS AND DISCUSSION

Our direct-write procedure is simple, involving basically three steps (see Figure 1 top). A Pd hexadecylthiolate film (~60 nm) spin-coated on a Si substrate was patterned using a 5 kV electron beam at 135 μC/cm^2 and developed in toluene for 10 s. The regions exposed to the e-beam remained on the substrate after developing (Figure 1), thus indicating the negative-tone resist behavior of the thiolate. Previous EBL work using thiolate species as a source of metal (Au) was restricted to functionalized polymeric resists, presumably due to processing difficulties, as alkylthiolates of most metals, once formed, cannot be easily solubilized. In contrast, Pd alkylthiolates are soluble in common organic solvents and can be self-assembled repeatedly.[35,36] Corresponding to the scanning electron microscopy (SEM) image of the four square areas (6.5 × 6.5 μm^2), the energy-dispersive spectral (EDS) images in Figure 1b–d show, as expected, the presence of Pd, C, and S, respectively, in the designated areas. The molar Pd:C:S value obtained for the patterned regions, 21:71:8, agrees with the initial composition (19:69.8:11.2) of the unexposed resist, $Pd(SC_{16}H_{35})_2$, implying that the electron dosage causes only minimal change in the overall composition.

Insight into the chemical nature of the Pd species in the patterned regions is gained by comparing its IR spectrum with those obtained while a Pd hexadecylthiolate film was subjected to thermolysis in air at different temperatures (Figure 2). The symmetric and antisymmetric methylene C–H stretching modes that appear at 2848 and 2918 cm^{-1}, respectively, for the pristine film exhibit, when heated, small positive shifts (~7 cm^{-1}) accompanied by diminished intensity, both foretelling the occurrence of defects, particularly gauche defects, in the hydrocarbon chains of the thiolate.[36] Palladium hexadecylthiolate is a lamellar structure (see schematic diagram in Figure 2) with alkyl chains predominately in the all trans-conformation with a bilayer thickness of 44.41 Å.[35] Under the given electron beam conditions (5 kV, 135 μC/cm^2), the hydrocarbon chains seem to develop defects and produce a disordered phase[37] that exhibits absorption bands somewhat resembling those obtained with the film subjected to 200 °C heating. The electron beam may

also promote radical formation and cross-linking of the alkyl chains.[15,37] The SEM image in Figure 3a shows the patterned area in Figure 1a after *ex situ* thermolysis at 230 °C. Pd M EDS map (Figure 3b) shows the presence of Pd in the designated region similar to that in Figure 1b. However, C K and S K signals became significantly weaker (Pd:C:S, 90:9.6:0.4) following thermolysis (compare Figure 3 c,d with Figure 1c,d, respectively). Pd thiolate, like other noble and seminoble metal thiolates, is known to produce metal species from thermolysis.[38,39] Accordingly, the C−H stretching bands disappeared (see inset of Figure 3). It is noteworthy that the patterned Pd produced this way hosts the lowest carbon content (9.6%) as compared to other studies on Pd[17,18] as well as on Au[14] involving EBL.

Transmission electron microscopy (TEM) analysis was carried out on a patterned region before and after thermolysis. For this purpose, a Cu holey grid was coated with the thiolate precursor, patterned with an electron beam (5 kV, 135 μC/cm^2), and developed in toluene. The TEM micrograph (Figure 4a) showed very small nanoparticles (<5 nm) with diffused rings in electron diffraction (see inset of Figure 4a). Following thermolysis at 230 °C, the particle size increased, 5–15 nm, due to agglomeration (Figure 4b). The crystalline nature of the nanoparticles is evident from the diffraction data (for details, see Supporting Information) and the high-resolution image shown in the insets of Figure 4b. Figure 4c,d shows respectively SEM and STEM images of the thermolyzed pattern (shown in the center), where a widely spread network of well-connected Pd nanoparticles is seen. This is essentially the origin of the mesoscalar electrical behavior.

The electrical behavior during thermolysis was examined by fabricating a circuit with a patterned thiolate line as an active element between Au gap electrodes on a SiO_2(150 nm)/Si substrate and collecting the $I-V$ data during heating (Figure 5a). We found that the current prior to thermolysis was in the range of picoamperes which, upon heating to 180 °C, increased to a few nanoamperes and, at 200 °C, to 0.1 mA (at 2 V). At 215 °C, the current was unsteady and increased by an order magnitude over a period of 120 s (see the lines labeled 215a, 215b, and 215c). At 230 °C, however, the current in the circuit shot up to 100 μA within 1 mV. Prior to thermolysis, the resistance of the Pd nanowire was ~11.2 MΩ, which gradually decreased to 0.65 kΩ when the wire was heated to 215 °C (see Figure 5b), beyond which the fall in resistance was steep, reaching a value of 20 Ω at 230 °C, corresponding to a specific resistivity of 0.300 $\mu\Omega$m. It is worth noting that this value of resistivity is only about 3 times the bulk Pd resistivity (0.105 $\mu\Omega$m). The highly conducting nature of the Pd nanowire obtained in our study is evident when compared to literature values of 100 and 417 $\mu\Omega$m from Stark *et al.*[12] and Reetz *et al.*,[17] respectively. The temperature-dependent resistivity for such a nanowire

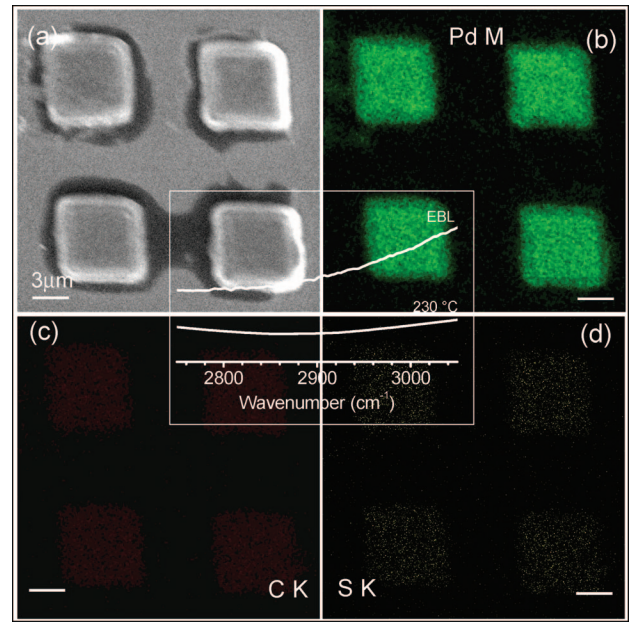

Figure 3. (a) SEM image and (b−d) EDS maps of the patterned film in Figure 1, after thermolysis at 230 °C for 20 min. The inset shows the FTIR spectra after thermolysis of both the patterned and the pristine films. The spectra are similar and are devoid of C−H stretches.

is expected to follow a linear behavior (see Supporting Information, Figure S1).

We have been able to reproducibly generate patterns of nanometric dimensions (Figure 6). In Figure 6a, we show a few line patterns of width ~30 nm. As mentioned earlier, our Pd thiolate resist is highly sensitive to the electron beam, and that makes large-area patterning with EBL more realistic. For example, the 250 × 230 μm^2 patterned square in Figure 6b was gener-

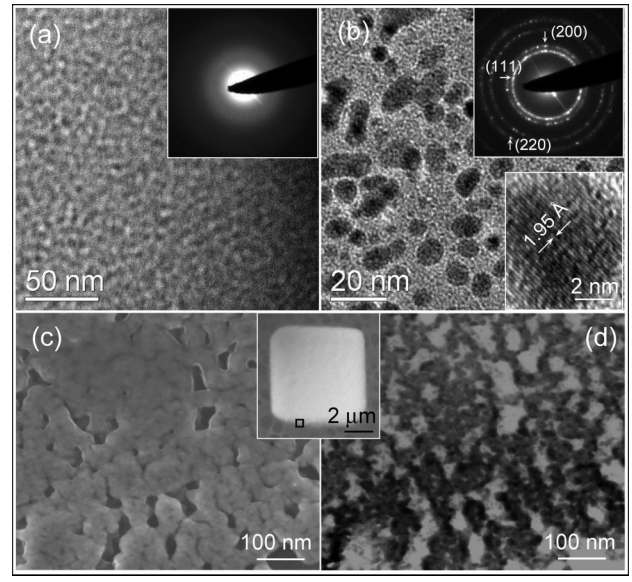

Figure 4. TEM images of patterned Pd before (a) and after (b) thermolysis, along with the corresponding ED data in the insets. The bottom inset in panel b shows a typical HRTEM image of a Pd nanoparticle. The marked *d*-spacing corresponds to *d*(200) of crystalline Pd (JCPDS no. 461043). SEM (c) and STEM (d) images from a Pd pattern (square region marked in the inset) after thermolysis.

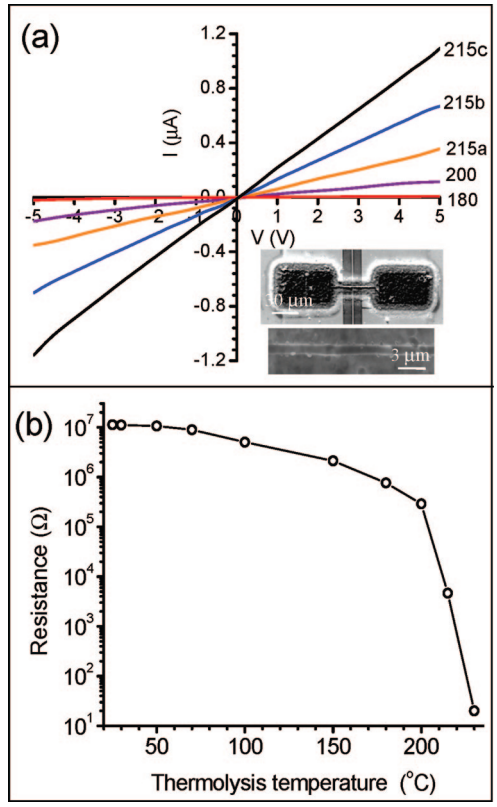

Figure 5. (a) *I*–*V* data of a patterned Pd hexadecylthiolate nanowire between 40 μm Au gap electrodes on a SiO_2(150 nm)/Si substrate subjected to different temperatures (in °C). At 215 °C, three measurements (lines labeled 215a, 215b, and 215c) were made within a span of 120 s. The insets show SEM images of the fabricated circuit. (b) Semilog plot of resistance (at 2 V) *versus* thermolysis temperature.

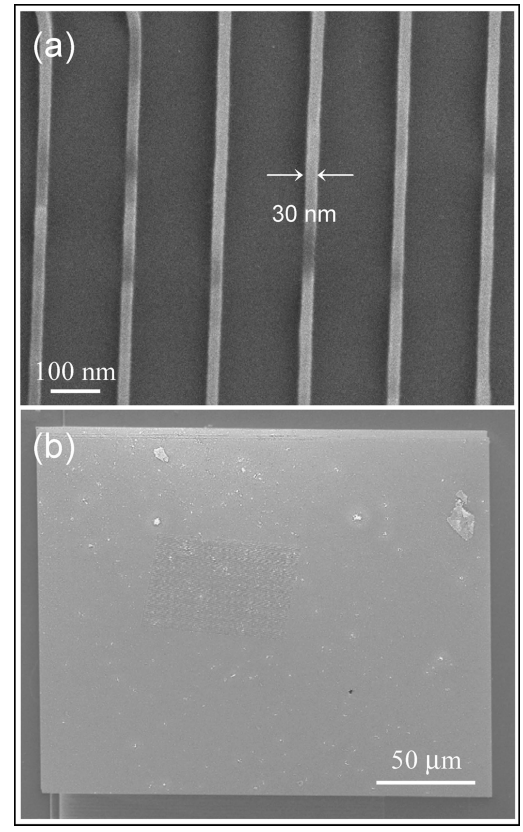

Figure 6. SEM images showing (a) thermolyzed Pd nanowires and (b) a large-area pattern (250 × 230 μm^2).

ated with an e-dosage as small as 36 $\mu C/cm^2$, which also corresponds to its sensitivity. It may be noted that the e-dosage used to create this pattern is much less that the commonly used e-dosages for metals, in particular for Pd, the literature values being 10^3 and 2×10^5 $\mu C/cm^2$ from Stark *et al.*[12] and Reetz *et al.*,[17] respectively.

CONCLUSION

In conclusion, the present study demonstrates the use of Pd hexadecylthiolate as a direct-write electron resist capable of producing nanometric patterns. The high solubility of the thiolate precursor qualifies it for processing as a resist. The resist preparation is simple, and EBL patterning involves only three steps: coating the resist, exposing, and developing. Being a molecular precursor, it allows high-resolution patterning and, importantly, requires very small dosages (~a few tens of $\mu C/cm^2$ at 5 kV), as the alkyl chains undergoing disorder and cross-linking are very sensitive to the energetic electrons. Post-treatment leading to metallic nanopatterns is simple, involving heating to 230 °C in air. While the composition of the patterned resist closely resembles that of the thiolate precursor, following thermolysis, the obtained metal lines contain carbon at a record low level (<10%), unusual in EBL studies. Although nanogranular in morphology, the patterns are mesoscopically metallic with a specific resistivity of 0.300 $\mu\Omega$m, definitely close to the bulk value (0.105 $\mu\Omega$m). The above advantages should encourage researchers to adopt the present recipe potentially for making metallic interconnects in nanocircuitry. The post-treatment temperature (230 °C) being favorable in circuit design, the thiolate precursor may also serve as a nanosolder. Further, intermittent temperature treatments may be useful if active elements of desired resistances (from megaohms to a few ohms) are to be obtained (see Figure 5b).

EXPERIMENTAL SECTION

The procedure adopted by us for the synthesis of the direct-write resist is as follows. To 5.0 mmol of $Pd(OAc)_2$ (Sigma Aldrich) in toluene (7 mL) was added 5.0 mmol of hexadecylthiol in toluene (3 mL), and the resulting mixture was stirred vigorously. Following the reaction, the solution became viscous, and the yellow color deepened to orange-yellow. The obtained thiolate was washed with methanol and acetonitrile to remove excess thiol and finally dissolved in toluene to obtain a 0.1 mM solution. For EBL, Si(111) substrates (n-doped, 4–7 $\Omega \cdot$cm) were cleaned by sonicating in acetone and double-distilled water and dried under flowing argon. The resist film (60 nm thick) was

made by spin-coating 30 μL of the Pd thiolate solution at 2000 rpm. EBL was performed using a Nova NanoSEM 600 instrument (FEI Co., The Netherlands). The electron beam energy employed for patterning was 5 kV. For nanocircuit fabrication, oxidized Si wafers with oxide thickness 150 nm were used. Thickness measurements were performed using a Stylus profiler Dektak 6M (Veeco, USA). Au metal film of 70 nm thickness was thermally deposited with a gap of 40 μm between the two electrodes. Energy-dispersive spectroscopy (EDS) analysis was performed with an EDAX Genesis instrument (Mahwah, NJ) attached to the SEM column. The EDS mapping was performed at 10 kV (energy window, 10 eV) with a beam current of 1.1 nA, the dwell time per pixel being 30 μs for a horizontal scan width of 30 μm. Transmission electron microscopy (TEM) measurements were carried out with a JEOL-3010 instrument operating at 300 kV ($\lambda = 0.0196$ Å) and a camera length 20 cm (calibrated with respect to the standard polycrystalline Au thin film). Fourier transform infrared measurements were done using a Bruker IFS66v/s spectrometer with a resolution of $\sim$2 cm^{-1}.

Acknowledgment. The authors are grateful to Professor C. N. R. Rao for his encouragement. Support from the Department of Science and Technology, Government of India, is gratefully acknowledged.

Supporting Information Available: Four-probe resistivity measurements and indexing of the ED and XRD patterns of the thermolyzed Pd film. This material is available free of charge *via* the Internet at http://pubs.acs.org.

REFERENCES AND NOTES

1. Gates, B. D.; Xu, Q.; Stewart, M.; Ryan, D.; Willson, C. G.; Whitesides, G. M. New Approaches to Nanofabrication: Molding, Printing, and Other Techniques. *Chem. Rev.* **2005**, *105*, 1171–1196.
2. Tseng, A. A. Recent Developments in Nanofabrication Using Focused Ion Beams. *Small* **2005**, *1*, 924–939.
3. Lin, J. F.; Bird, J. P.; Rotkina, L.; Bennett, P. A. Classical and Quantum Transport in Focused-Ion-Beam-Deposited Pt Nanointerconnects. *Appl. Phys. Lett.* **2003**, *82*, 802–804.
4. Tham, D.; Nam, C. Y.; Fischer, J. E. Microstructure and Composition of Focused-Ion-Beam-Deposited Pt Contacts to GaN Nanowires. *Adv. Mater.* **2006**, *18*, 290–294.
5. Brintlinger, T.; Fuhrer, M. S.; Melngailis, J.; Utke, I.; Bret, T.; Perentes, A.; Hoffmann, P.; Abourida, M.; Doppelt, P. Electrodes for Carbon Nanotube Devices by Focused Electron Beam Induced Deposition of Gold. *J. Vac. Sci. Technol. B* **2005**, *23*, 3174–3177.
6. De Marzi, G.; Lacopino, D.; Quinn, A. J.; Redmond, G. Probing Intrinsic Transport Properties of Single Metal Nanowires: Direct-write Contact Formation Using a Focused Ion Beam. *J. Appl. Phys.* **2004**, *96*, 3458–3462.
7. Valizadeh, S.; Abid, M.; Hernández-Ramírez, F.; Rodríguez, A. R.; Hjort, K.; Schweitz, J. A. Template Synthesis and Forming Electrical Contacts to Single Au Nanowires by Focused Ion Beam Techniques. *Nanotechnology* **2006**, *17*, 1134–1139.
8. Im, Y.; Lee, C.; Vasquez, R. P.; Bangar, M. A.; Myung, N. V.; Menke, E. J.; Penner, R. M.; Yun, M. Investigation of a Single Pd Nanowire for Use as a Hydrogen Sensor. *Small* **2006**, *2*, 356–358.
9. Kind, H.; Bonard, J. M.; Emmenegger, C.; Nilsson, L. O.; Hernadi, K.; Maillard-Schaller, E.; Schlapbach, L.; Forró, L.; Kern, K. Patterned Films of Nanotubes Using Microcontact Printing of Catalysts. *Adv. Mater.* **1999**, *11*, 1285–1289.
10. Lee, J. Y.; Yin, D.; Horiuchi, S. Site and Morphology Controlled ZnO Deposition on Pd Catalyst Prepared from Pd/PMMA Thin Film Using UV Lithography. *Chem. Mater.* **2005**, *17*, 5498–5503.
11. Corbierre, M. K.; Beerens, J.; Lennox, R. B. Gold Nanoparticles Generated by Electron Beam Lithography of Gold(I)-Thiolate Thin Films. *Chem. Mater.* **2005**, *17*, 5774–5779.
12. Stark, T. J.; Mayer, T. M.; Griffis, D. P.; Russell, P. E. Electron Beam Induced Metallization of Palladium Acetate. *J. Vac. Sci. Technol. B* **1991**, *9*, 3475–3478.
13. Chan, W. Y.; Clendenning, S. B.; Berenbaum, A.; Lough, A. J.; Aouba, S.; Ruda, H. E.; Manners, I. Highly Metallized Polymers: Synthesis, Characterization, and Lithographic Patterning of Polyferrocenylsilanes with Pendant Cobalt, Molybdenum, and Nickel Cluster Substituents. *J. Am. Chem. Soc.* **2005**, *127*, 1765–1772.
14. Hoffmann, P.; Assayag, G. B.; Gierak, J.; Flicstein, J.; Maar-Stumm, M.; van den Bergh, H. Direct Writing of Gold Nanostructures Using a Gold-Cluster Compound and a Focused-Ion Beam. *J. Appl. Phys.* **1993**, *74*, 7588–7591.
15. Werts, M. H. V.; Lambert, M.; Bourgoin, J. P.; Brust, M. Nanometer Scale Patterning of Langmuir-Blodgett Films of Gold Nanoparticles by Electron Beam Lithography. *Nano Lett.* **2002**, *2*, 43–47.
16. Griffith, S.; Mondol, M.; Kong, D. S.; Jacobson, J. M. Nanostructure Fabrication by Direct Electron-Beam Writing of Nanoparticles. *J. Vac. Sci. Technol. B* **2002**, *20*, 2768–2772.
17. Reetz, M. T.; Winter, M.; Dumpich, G.; Lohau, J.; Friedrichowski, S. F. Fabrication of Metallic and Bimetallic Nanostructures by Electron Beam Induced Metallization of Surfactant Stabilized Pd and Pd/Pt Clusters. *J. Am. Chem. Soc.* **1997**, *119*, 4539–4540.
18. Lohau, J.; Friedrichowski, S.; Dumpich, G.; Wassermann, E. F.; Winter, M.; Reetz, M. T. Electron-Beam Lithography with Metal Colloids: Direct Writing of Metallic Nanostructures. *J. Vac. Sci. Technol. B* **1998**, *16*, 77–79.
19. Ross, I. M.; Luxmoore, I. J.; Cullis, A. G.; Orr, J.; Buckle, P. D.; Jefferson, J. H. Characterisation of Tungsten Nano-wires Prepared by Electron and Ion Beam Induced Chemical Vapour Deposition. *J. Phys.: Conf. Ser.* **2006**, *26*, 363–366.
20. Kunz, R. R.; Mayer, T. M. Electron Beam Induced Surface Nucleation and Low-Temperature Decomposition of Metal Carbonyls. *J. Vac. Sci. Technol. B* **1988**, *6*, 1557–1564.
21. Rotkina, L.; Oh, S.; Eckstein, J. N.; Rotkin, S. V. Logarithmic Behavior of the Conductivity of Electron-Beam Deposited Granular Pt/C Nanowires. *Phys. Rev. B* **2005**, *72*, 233407–4.
22. Koops, H. W. P.; Schössler, C.; Kaya, A.; Weber, M. Conductive Dots, Wires, and Supertips for Field Electron Emitters Produced by Electron-Beam Induced Deposition on Samples Having Increased Temperature. *J. Vac. Sci. Technol. B* **1996**, *14*, 4105–4109.
23. Botman, A.; Mulders, J. J. L.; Weemaes, R.; Mentink, S. Purification of Platinum and Gold Structures After Electron-Beam-Induced Deposition. *Nanotechnology* **2006**, *17*, 3779–3785.
24. Barry, J. D.; Ervin, M.; Molstad, J.; Wickenden, A.; Brintlinger, T.; Hoffman, P.; Meingailis, J. Electron Beam Induced Deposition of Low Resistivity Platinum from $Pt(PF_3)_4$. *J. Vac. Sci. Technol. B* **2006**, *24*, 3165–3168.
25. Utke, I.; Hoffmann, P.; Dwir, B.; Leifer, K.; Kapon, E.; Doppelt, P. Focused Electron Beam Induced Deposition of Gold. *J. Vac. Sci. Technol. B* **2000**, *18*, 3168–3171.
26. Prestigiacomo, M.; Bedu, F.; Jandard, F.; Tonneau, D.; Dallaporta, H.; Roussel, L.; Sudraud, P. Purification and Crystallization of Tungsten Wires Fabricated by Focused-Ion-Beam-Induced Deposition. *Appl. Phys. Lett.* **2005**, *86*, 192112–192113.
27. Puretz, J.; Swanson, L. W. Focused Ion Beam Deposition of Pt Containing Films. *J. Vac. Sci. Technol. B* **1992**, *10*, 2695–2698.
28. Tao, T.; Ro, J.; Melngailis, J.; Xue, Z.; Kaesz, H. D. Focused Ion Beam Induced Deposition of Platinum. *J. Vac. Sci. Technol. B* **1990**, *8*, 1826–1829.
29. Peñate-Quesada, L.; Mitra, J.; Dawson, P. Non-linear Electronic Transport in Pt Nanowires Deposited by Focused Ion Beam. *Nanotechnology* **2007**, *18*, 215203(5 pp).
30. Telari, K. A.; Rogers, B. R.; Fang, H.; Shen, L.; Weller, R. A.; Braski, D. N. Characterization of Platinum Films Deposited by Focused Ion Beam-assisted Chemical Vapor Deposition. *J. Vac. Sci. Technol. B* **2002**, *20*, 590–595.

31. Yan, J.; Gupta, M. C. Direct Metal Pattern Writing by VUV Photodissociation. *J. Vac. Sci. Technol. B* **2004**, *22*, 3202–3205.
32. Yin, D.; Horiuchi, S.; Morita, M.; Takahara, A. Tunable Metallization by Assembly of Metal Nanoparticles in Polymer Thin Films by Photo- or Electron Beam Lithography. *Langmuir* **2005**, *21*, 9352–9358.
33. Geissler, M.; Wolf, H.; Stutz, R.; Delamarche, E.; Grummt, U. W.; Michel, B.; Bietsch, A. Fabrication of Metal Nanowires Using Microcontact Printing. *Langmuir* **2003**, *19*, 6301–6311.
34. Wolfe, D. B.; Love, J. C.; Paul, K. E.; Chabinyc, M. L.; Whitesides, G. M. Fabrication of Palladium-based Microelectronic Devices by Microcontact Printing. *Appl. Phys. Lett.* **2002**, *80*, 2222–2224.
35. Thomas, P. J.; Lavanya, A.; Sabareesh, V.; Kulkarni, G. U. Self-Assembling Bilayers of Palladiumthiolates in Organic Media. *Proc. Indian Acad. Sci. (Chem. Sci.)* **2001**, *113*, 611–619.
36. John, N. S.; Thomas, P. J.; Kulkarni, G. U. Self-Assembled Hybrid Bilayers of Palladium Alkanethiolates. *J. Phys. Chem. B* **2003**, *107*, 11376–11381.
37. Seshadri, K.; Froyd, K.; Parikh, A. N.; Allara, D. L.; Lercel, M. J.; Craighead, H. G. Electron-Beam-Induced Damage in Self-Assembled Monolayers. *J. Phys. Chem.* **1996**, *100*, 15900–15909.
38. Carotenuto, G.; Martorana, B.; Perlo, P.; Nicolais, L. A Universal Method for the Synthesis of Metal and Metal Sulfide Clusters Embedded in Polymer Matrices. *J. Mater. Chem.* **2003**, *13*, 2927–2930.
39. John, N. S. Ph.D. Thesis, Investigations of Metal and Metal-Organic Bilayer Nanostructures Employing Atomic Force Microscopy and Related Techniques; Jawaharlal Nehru Centre for Advanced Scientific Research, Bangalore, 2007 (620.11 P07); pp 113–119..